

Tensile shear load in resistance spot welding of dissimilar metals: An optimization study using response surface methodology

Sukarman^{1,2*}, Triyono¹, Budi Kristiawan¹, Amir², Nazar Fazrin², Ade Suhara², Renata Lintang Azizah³, Fajar Mucharom⁴

¹ Department of Mechanical Engineering, Faculty of Engineering, Universitas Sebelas Maret, 57126 Surakarta, Central Java, **Indonesia**

² Department of Mechanical Engineering, Faculty of Engineering, Universitas Buana Perjuangan Karawang, 41151 Karawang, West Java, **Indonesia**

³ Department of Mechanical Engineering Education, Faculty of Technology and Vocational Education Universitas Pendidikan Indonesia, 40154 Bandung, West Java, **Indonesia**

⁴ Department of Engineering Science, Faculty of Engineering, Duisburg-Essen University, Forsthausweg 2 Duisburg 47057, North Rhine Westphalia, **Germany**

✉ sukarman@ubpkarawang.ac.id

This article contributes to:



Highlights:

- The influence of using dissimilar materials in resistance spot welding (RSW) was studied to optimize tensile strength load (TSL).
- Response surface methodology (RSM) and Box-Behnken were implemented to achieve the desired outcome and determine the input parameters.
- The RSW process had a significant influence on the enhancement of productivity across industries.

Abstract

Resistance spot welding (RSW) is being applied extensively in different industries, specifically the automotive sector. Therefore, this study was conducted to optimize the tensile strength load (TSL) in RSW by investigating the application of dissimilar materials as input parameters. The optimization process involved the combination of different galvanized and non-galvanized steel materials. The production of car bodies using galvanized steel with approximately 13.0 microns thick zinc (Zn) coating was found to be a standard practice, but this zinc layer usually presents challenges due to the poor weldability. This study prepared 27 units of TSL samples using a spot-welding machine and a pressure force system (PFS) for the electrode tip. The aim was to determine the optimal TSL through the exploration of specified RSW parameters. The process focused on using the response surface methodology (RSM) to achieve the desired outcome while the Box-Behnken design was applied to determine the input parameters. The optimal TSL obtained was 5265.15 N by setting the squeeze time to 21.0 cycles at a welding current of 24.5 kA, a welding time of 0.5 s, and a holding time of 15.0 cycles. The highest TSL value recorded was 5937.94 N at 21.0 cycles, 27.0 kA, 0.6 s, and 15.0 cycles respectively. These findings were considered significant to the enhancement of productivity across industries, specifically in the RSW process. However, further study was required to investigate additional response variables such as the changes in hardness and microstructure.

Keywords: Box-Behnken design, Resistance spot welding, Response surface methodology, Tensile shear load

Article info

Submitted:
2023-07-10

Revised:
2023-07-28

Accepted:
2023-07-29



This work is licensed under a Creative Commons Attribution-NonCommercial 4.0 International License

Publisher

Universitas Muhammadiyah
Magelang

1. Introduction

Resistance spot welding (RSW) is welding technology a widely utilized in the automotive industry, particularly to assemble car body components [1]. It is the preferred method to join steel

body structures in automobile manufacturing, with an average of approximately 5,000 welding points per car during assembly [2]. The high demand for spot welds indicates the significance of RSW in the automotive sector [3], [4]. It has also been noted that galvanized steel coated with zinc (Zn) provides excellent corrosion resistance but poses some challenges associated with weldability, specifically when joining galvanized steel with non-galvanized steel such as in the outer and inner panels of the car body as indicated in Figure 1 [5]. The disparity in melting points between the zinc coating and non-galvanized steel also presents a hurdle in achieving efficient and flawless RSW. These improper welding parameter settings can lead to welds that fail to meet the required standards during the production process. Therefore, there is a need to ensure appropriate parameters are selected to achieve reliable and high-quality spot welds [6]. The efforts to address this challenge are essential for the optimization of RSW processes and the enhancement of the overall welding efficiency in the automotive manufacturing industry [7]. Several metal joining techniques are commonly used in manufacturing processes such as the RSW, Gas Tungsten Arc Welding (GTAW), and Shielded Metal Arc Welding (SMAW). The differences identified in the combination of materials using the RSW and GMAW/SMAW methods are presented in the following Figure 2 [8], [9].

RSW is a type of metal welding that joins two or more metal surfaces together using current resistance as a heat source. The process involves the resistance of electricity heating the metal surfaces to melt and fuse at the welding site [10], [11]. The subsection of the metal welding contacts to the heat produced by electric resistance usually leads to the melting of the metals [12]. The RSW process is normally conducted within a specific cycle time using several parameters such as the welding current and time as well as the electrode force [13]. Moreover, the electric resistance often develops at the surface where the electrode and metal plate come into contact. However, water cooling was required at the ends of the electrode to prevent the whole metal from melting. The schematic representation of the RSW process is presented in the following Figure 3 to visualize the setup and the critical components [8], [14].

Metal fusion usually occurs through a combination of heat and pressure exerted on the metal surfaces to be joined from both ends of the electrodes. In the RSW process, pressure is applied throughout the welding cycle to achieve a certain goal [15]–[17] which is to shape the metal in the nugget area after heating and prevent deformation or warping of the joint. This pressing stage starts at the squeeze time cycle and the welding occurs when current flows through the tip of the electrode to generate heat and cause fusion between the metal surfaces being joined [16].



Figure 1.
The outer and inner panels of the car body

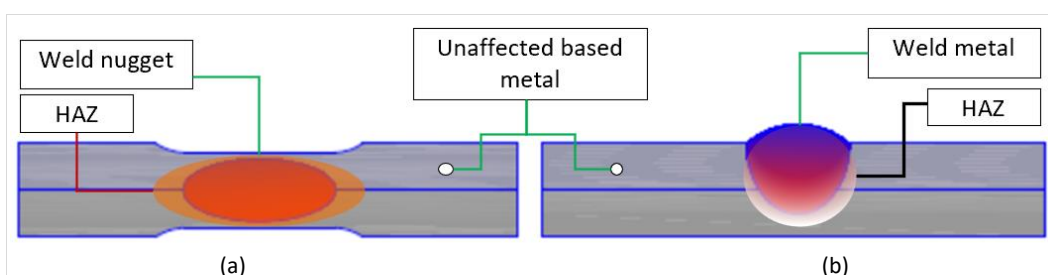
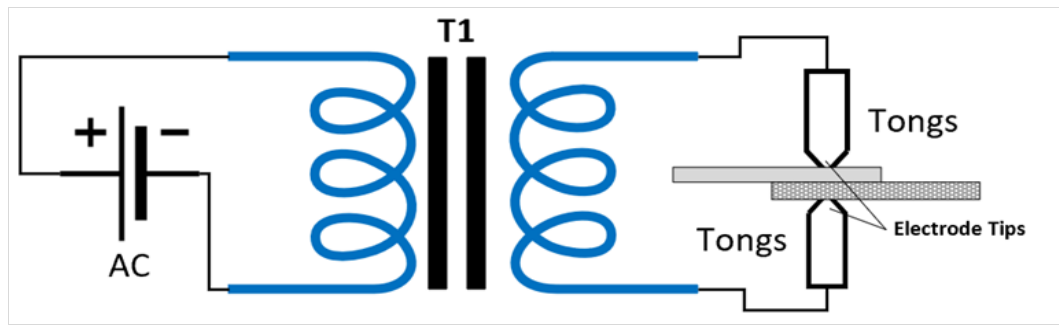


Figure 2.
The comparison of weld seams from (a) RSW and (b) GMAW results

Figure 3.
The schematic
of the resistance spot
welding machine



Recent publications on the mechanical properties of the steel welded through the RSW technique often focus on examining a single type of steel. For example, Thakur and Nandedkar attempted to optimize RSW parameters specifically for galvanized steel sheets using RSM with parameters such as preheating current, squeeze time, weld time, hold time, and electrode pressure. ANOVA was applied for analysis using TSL as the optimized response parameter and the results showed that welding current and time parameters had a significant impact on the TSL [18]. Another study by Shafee et al. investigated RSW using low-carbon steel materials with thicknesses of 0.8 mm and 1.0 mm. A 3-parameter and 3-level experimental design including electrode force, welding current, and welding time was employed based on the RSM. The direct-tensile strength and TSL were analyzed using larger-is-better data features for the signal-to-noise ratios and the results showed that welding current and time were the main factors affecting TSL [19].

Emre et al. investigated the RSW optimization of TRIP800 steel using the two-way ANOVA method with welding current and time as input parameters. A 5-level approach was utilized for the welding time and a 7-level approach for the welding current. Moreover, two response variables evaluated include the geometric nuggets and TSL, and the results showed that the nugget diameter and size ratio should be at least $4.5Vt$ and within the range of 0.15-0.30, respectively, for TRIP800 steel. These requirements were found to be important to achieve the desired pull-out failure mode, surface quality of weld area, and TSL [20]. Vignesh et al. also conducted an optimization study on the RSW parameter by combining 316L SUS and 2205 duplex SUS. The process involved using three variables including the welding current, electrode tip diameter, and the heating cycle. The objective of the optimization was to maximize the TSL values, which was an important indicator of joint strength in RSW. The analysis was conducted using ANOVA and the results showed that the welding current, heating cycle, and electrode tip diameter had a significant effect on the TSL values [21].

The focus of this RSW study was to join two distinct materials, low-carbon hot-rolled mild steel plates, sheets, and strips (SPHC, JIS 3131) with galvanized steel of hot-dip galvanized steels (SGCC, JIS 3302). These materials have distinct properties primarily associated with the zinc (Zn) coating on the SGCC steel which subsequently has a significant impact on its weldability [22]. An experimental approach in the form of RSM was adopted to analyze and optimize the RSW process. The parameters considered were the pressing time, welding current, welding time, and holding time. The RSM approach facilitated the optimization of these input variables by considering their minimum and maximum values. The primary goal was to establish the ideal TSL value to prevent interfacial failure mode and boost the overall effectiveness of the welding process by identifying the critical parameters and their corresponding values. The RSM led to the successful identification of the minimum parameter values to be implemented to avoid interfacial failure mode. This finding provides valuable insights for optimizing the RSW process and enhancing its reliability and efficiency.

2. Methods

2.1. Material and Testing Procedure

This study utilized two types of galvanized and non-galvanized materials, SPHC and SGCC, with different thicknesses of 3.0 mm and 0.8 mm, respectively. The SGCC is a galvanized steel plate that belongs to the cold rolled coil (CRC) category. It is galvanized and annealed using the SPHC plate as the base material and is widely employed in several manufacturing industries due to its favorable properties [18]. Detailed information on the chemical composition and materials used in this study

is presented in Table 1 while the mechanical properties of the SPHC materials as well as their characteristics and behavior under specific conditions are indicated in Table 2 [23].

Table 1.

The chemical composition of galvanized steel and SHPC (%)

Element	Galvanized steel (SGCC)		SPHC [24]	
	JIS G3302 [25]	CSV4505B*	JIS 3131 [26]	SP51023*
C	≤ 0.15	0.0063	≤ 0.15	0.0364
Mn	≤ 0.08	0.1940	≤ 0.06	0.0192
S	≤ 0.05	0.0043	≤ 0.05	0.005
P	≤ 0.05	0.0017	≤ 0.05	0.0011

*Mill certificate

Table 2.

The mechanical properties and materials standard

Mechanical Properties	(SGCC)		SPHC [24]	
	JIS G3302 [25]	CSV4505B*	JIS 3131 [26]	SP51023*
YP (N/mm ²)	≤ 205	231.0	≥ 240	195.0
TS (N/mm ²)	≤ 270	333.0	≤ 270	315.0
EL (%)	-	45.0	≤ 37	45.2

*Mill certificate

The specimens were prepared through a shearing process with the SPCC and SPHC plate sheets cut at 40 x 105 mm [27]. The RSW process was implemented by placing two pieces of material to be spot welded in the right position. Efforts were made to ensure the surfaces were in good contact without any gaps. Moreover, the galvanized steel was placed on top of the joint while the non-galvanized steel was at the bottom. This arrangement was used to determine the effect of the input parameter on the zinc layer coating the surface of galvanized steel. The joining method overlapped with the geometric dimensions according to Figure 4.

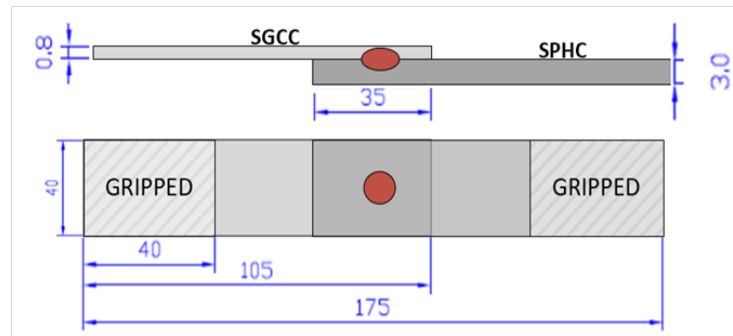


Figure 4. The geometry of RSW specimens

The metal surfaces were subjected to the heat produced through electrical resistance and melted. An RSW machine with a 35 kVA capacity was used for this purpose while a pneumatic system with a pressure of 3.5 MPa was applied to regulate the pressure to the tip ends of the electrodes. Moreover, a pointed electrode was utilized with a bottom diameter of 8 mm and a top radius of 2.5 mm [10], [17]. The pressure force exerted on the electrode tip was calculated using Eq. (1) [28].

$$F = P \cdot A \quad (1)$$

where, F stands for force (N), P for pressure (N/m²), and A for cross-sectional area (m²). Equation (1) was used to determine the compressive force delivered to both tip ends of the electrode with the top radius recorded to be 2.5 mm and the pressure being 68.7 N.

There are generally two failure modes in the application of RSW for metal joining, and these include the pull-out and interfacial modes. The interfacial mode usually occurs when the diameter of the nuggets formed is smaller than the required minimum [8], [15] or when there is insufficient fusion between the materials during the welding process, mostly due to poor welding practices [8], [9]. Insufficient fusion can also be associated with the difference in melting points between zinc in galvanized and non-galvanized steel materials [29]. Meanwhile, the pull-out failure mode is desirable because it indicates a more substantial connection than the base metals, and it is usually the target in RSW. It is also important to meet the minimum nugget diameter and this can be achieved using the following Eq. (2). [30].

$$D_{min} = 4.5 \sqrt{t} \quad (2)$$

where, "t" represents the minimum thickness of the connected metals which is 0.8 mm for SGCC and 3.0 mm for SPHC materials. According to equation (2), the required minimum nugget diameter

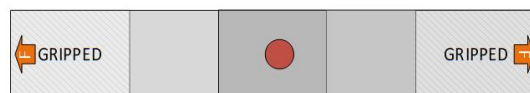
was calculated to be 4.27 mm. Therefore, the experiment was conducted using a 5.0 mm diameter electrode. The RSW machine utilized in this study is presented in [Figure 5](#).



Figure 5.
The RSW machine with a power capacity of 35 kW [24]

2.2. Tensile Shear Load

Tensile shear load (TSL) is a measure of the strength of the joint between two materials being spot welded. It can be tested using a special tensile shear test where the specimen from the RSW process is placed between the test devices and subjected to a tensile force perpendicular to the welding direction.



This tensile force causes a load to act on the joint to test the strength of the joint. The TSL test was conducted in this study to determine the strength of each sample and this was achieved using the Shimadzu engine model AGS-X 10kN STD E200V with a capacity of 10,000 N [31]. The withdrawal speed was managed at 35 mm/min and the process was conducted as indicated in [Figure 6](#).



Figure 6.
Tensile shear load test of the coupon on UTM

2.3. Box-Behnken Design and Input Parameters

RSM technical with the Box-Behnken Design approach was used in this study and four input parameters were defined and selected to evaluate the performance of the RSM in metal welding galvanized and non-galvanized steels. The parameters were used to predict the characteristics of the RSW, specifically the welding strength. The parameters were independent variables that could be controlled independently, including the squeeze time, welding current, welding time, and holding time.

Each process parameter was also established and defined using statistical software with due consideration for the minimum and maximum limits specified by the RSW machine. However, it could be challenging to control the surface condition of the base metal and electrode temperature

in the RSW process. This led to the adoption of the Box-Behnken Design matrix as an RSM technique to optimize the tensile stress in metal joining. The matrix was applied based on the minimum and maximum value limits for each parameter, as shown in [Table 3](#).

Table 3.
Box-Behnken
design input parameter

Code	Welding Parameters	Units	Input Parameter	
			Min.	Max.
A	Squeeze time	Cycles*	18.0	22.0
B	Weld. current	kA	22.0	27.0
C	Weld. time	Second	0.4	0.6
D	Hold time	Cycles*	12.0	18.0

*1 cycle = 1/60 minutes [\[32\]](#), [\[33\]](#)

A total of 26 test iterations were observed after controlling the input parameters using the RSM approach and degenerating the minimum and maximum parameters from the Marik Box-Behnken Design (BBD) as indicated in [Table 4](#). The results also produced one total block and three center points which were used to identify the ideal TSL condition for each RSW parameter [\[32\]](#).

Table 4.
Matrix
experimental using
RSM approach
generated by statistical
software

Run	Std Order	Run Order	Pt Type	Squeeze Time	Weld. Current	Weld Time	Hold Time
1	4	1	2	22.0	27.0	0.5	15.0
2	20	2	2	22.0	24.5	0.6	15.0
3	3	3	2	20.0	27.0	0.5	15.0
4	14	4	2	21.0	27.0	0.4	15.0
5	8	5	2	21.0	24.5	0.6	18.0
6	22	6	2	21.0	27.0	0.5	12.0
7	13	7	2	21.0	22.0	0.4	15.0
8	11	8	2	20.0	24.5	0.5	18.0
9	16	9	2	21.0	27.0	0.6	15.0
10	18	10	2	22.0	24.5	0.4	15.0
11	10	11	2	22.0	24.5	0.5	12.0
12	24	12	2	21.0	27.0	0.5	18.0
13	12	13	2	22.0	24.5	0.5	18.0
14	7	14	2	21.0	24.5	0.4	18.0
15	17	15	2	20.0	24.5	0.4	15.0
16	6	16	2	21.0	24.5	0.6	12.0
17	1	17	2	20.0	22.0	0.5	15.0
18	21	18	2	21.0	22.0	0.5	12.0
19	27	19	0	21.0	24.5	0.5	15.0
20	19	20	2	20.0	24.5	0.6	15.0
21	15	21	2	21.0	22.0	0.6	15.0
22	2	22	2	22.0	22.0	0.5	15.0
23	23	23	2	21.0	22.0	0.5	18.0
24	9	24	2	20.0	24.5	0.5	12.0
25	5	25	2	21.0	24.5	0.4	12.0
26	25	26	0	21.0	24.5	0.5	15.0

2.4. The Response Surfaces and The Contour Plots

Response surfaces and contour plots are graphical representations used in statistical analysis to visualize the relationship between multiple variables and a response variable. These surfaces and plots are commonly employed in experimental design, optimization, and regression analysis [\[33\]](#). Response surfaces display the relationship between two or more independent variables and a dependent response variable [\[34\]](#). These surfaces are typically represented in three-dimensional plots, where the axes represent the independent variables, and the height or color indicates the response variable. The examination of the shape and patterns of the surface usually provides insights into the interactions and effects of the variables on the response.

The response surfaces and contour plots also allow the visual exploration of the relationships and interactions between variables, identification of optimum conditions, and making informed decisions regarding experimental design or parameter optimization [\[35\]](#). They serve as a valuable tool for understanding complex systems and optimizing processes in different scientific and engineering domains.

The contour plots normally provide a two-dimensional representation of the response surface [36]. The contour lines or color gradients indicate the values of the response variable at different combinations of the independent variables. The plots usually help to identify regions of optimal or desirable responses based on specific criteria or constraints.

3. Results and Discussion

3.1. Tensile Shear Load Analysis

The highest TSL was found in the 9th iteration to be 5937.94 N at the squeezed time of 21.0 cycles, welding current of 27.0 kA, welding time of 0.6 s, and holding time of 15.0 cycles as presented in Figure 7. Moreover, the ideal condition was achieved with a TSL of 5265.15 N which was recorded at 21.0 cycles, 24.5 kA, 0.5 s, and 1.05 cycles respectively.

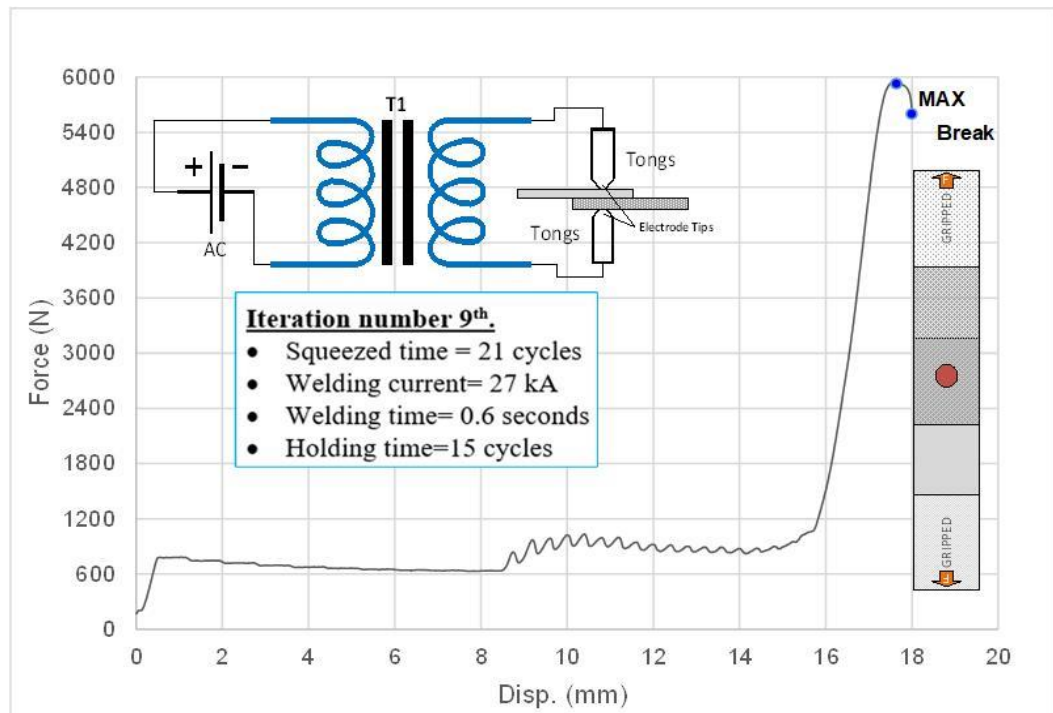


Figure 7.
The highest Tensile shear load achieved by RSM

The lowest TSL was recorded to be 4553.54 N in the 7th iteration at a squeeze time of 21 cycles, welding current of 22 kA, welding time of 0.4 s, and holding time of 15 cycles. The results showed that not all samples tested for TSL experienced pull-out failure mode. Interfacial failure was reported in 50% of the samples with a welding time of 0.4 s, specifically in iterations 7, 15, and 25 as presented in Figure 8. This indicated an occurrence of a perfect fusion process between the SGCC and SPHC metals, except for those welded at 0.4 s that exhibited satisfactory results in 50% of their samples. The phenomenon showed that the combination of parameters using welding time was not effective enough to melt the 18.5-micron zinc layer on the SGCC material [19].

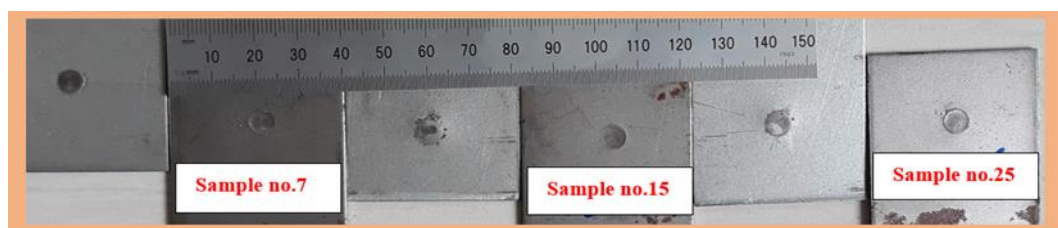


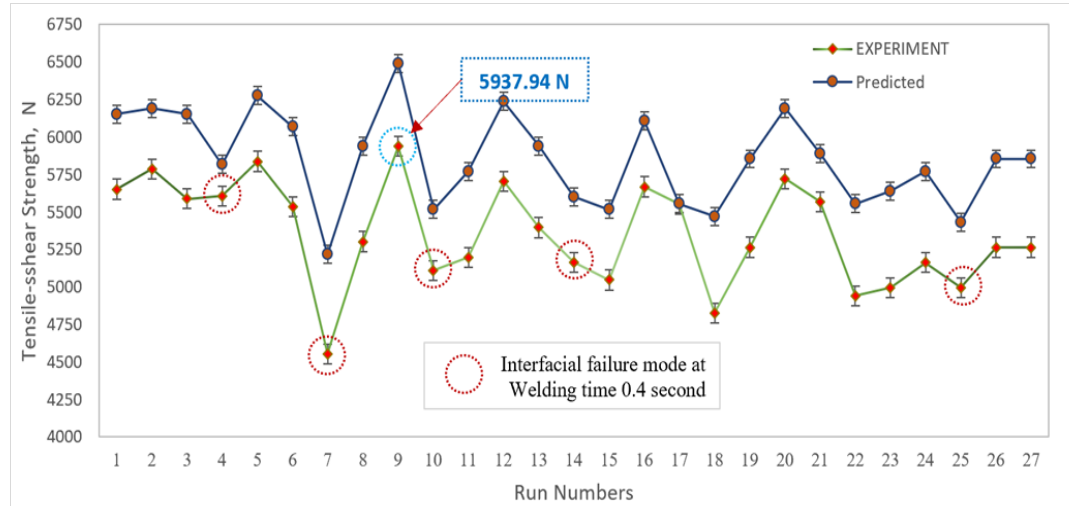
Figure 8.
Interfacial failure mode condition on sample numbers 7, 15, and 25

3.2. Regression Linear Analysis

Linear regression is commonly used for prediction, forecasting, and understanding the relationship between variables. This is due to its ability to provide insights into the strength and direction of the relationship and the significance of the independent variables in explaining the

variation in the dependent variable. The coefficients can also be used to make predictions or estimate the impact of changes in the independent variables on the dependent variable as presented in Figure 9. The statistical software package was applied to evaluate the multi-linear regressions of the TSL for the RSW. Meanwhile, it was suggested that the analysis be conducted based on the specific objective and functions of the software selected to generate and interpret linear regression models effectively. This led to the selection of the linear regression model provided in Eq. (3) to predict the TSL of RWS.

Figure 9. The Tensile shear load comparison between experimental and predictions



$$TSS_{SPHC-SGCC} = 822 - 24.0A + 119.6B + 3369C + 28.2 D \tag{3}$$

where *A* indicates squeeze time, *B* is welding current, *C* represents welding time, and *D* is the holding time.

3.3. The Analysis of Variance

The analysis of variance (ANOVA) results for the RSW responses generated through statistical software at a confidence interval for a mean estimated at 95% and analyzed based on their percent contribution using Eq. (4) are presented in Table 5 [19], [21]. This process was used to optimize the TSL response by evaluating the key variables. The contribution percentage also showed the extent to which the RSW parameters influenced the quality of the weld joint. The parameters with higher contribution percentages were believed to have a greater impact on the quality [9]. The results showed that welding current was the most significant parameter affecting the quality of the welded joint while welding time had the most minor significance.

$$\% \text{ contributions} = \frac{MS_i}{\sum MS} \times 100\% \tag{4}$$

where, *MS* indicates the mean sum of squares and subscript *i* represents the input parameters of RSW.

Table 5. Analysis of Variance for TSL-Galvanized steel vs. non-galvanized steel:

Parameters	DF	SS	MS	% Contribution
Squeeze Time	2	11380.534	5690.27	1.4%
Welding Current	6	1.36E+06	226981.0	55.6%
Welding Time	10	1.61E+06	160992.47	39.4%
Holding Time	6	86879.218	14479.87	3.5%

DF= degree of freedom, SS= the sum of squares, MS= mean sum of squares

Further analysis confirmed that the welding current contributed 55.6% followed by welding time at 39.4% while squeeze time had the lowest with 1.4%. In summary, a higher contribution percentage indicated a more decisive influence of the parameter on the quality of the welded joint. These findings were observed to be consistent with previous study by [35], and [37] that identified welding current as the most critical parameter in RSW. The estimated variance for these experiments was 0.09, indicating an acceptable experimental design.

3.4. Analysis of Response Surfaces and The Contour Plots

The order response surface model was developed using the four responses to determine the critical input parameters influencing the TSL. The design was expanded to evaluate more data points to increase the chances of identifying the ideal parameter combinations [35]. The center point in the design represented a set of experimental conditions and 27 independent experimental replicates were conducted to assess the variation across all designs. Moreover, the standard deviation was calculated based on the variation between these conditions. Each optimization experiment was randomly conducted within a single measurement block [37]. The optimal TSL recorded was 5265.15 N at the center of the response surface. The response surface of the TSL is presented in the following Figure 10.

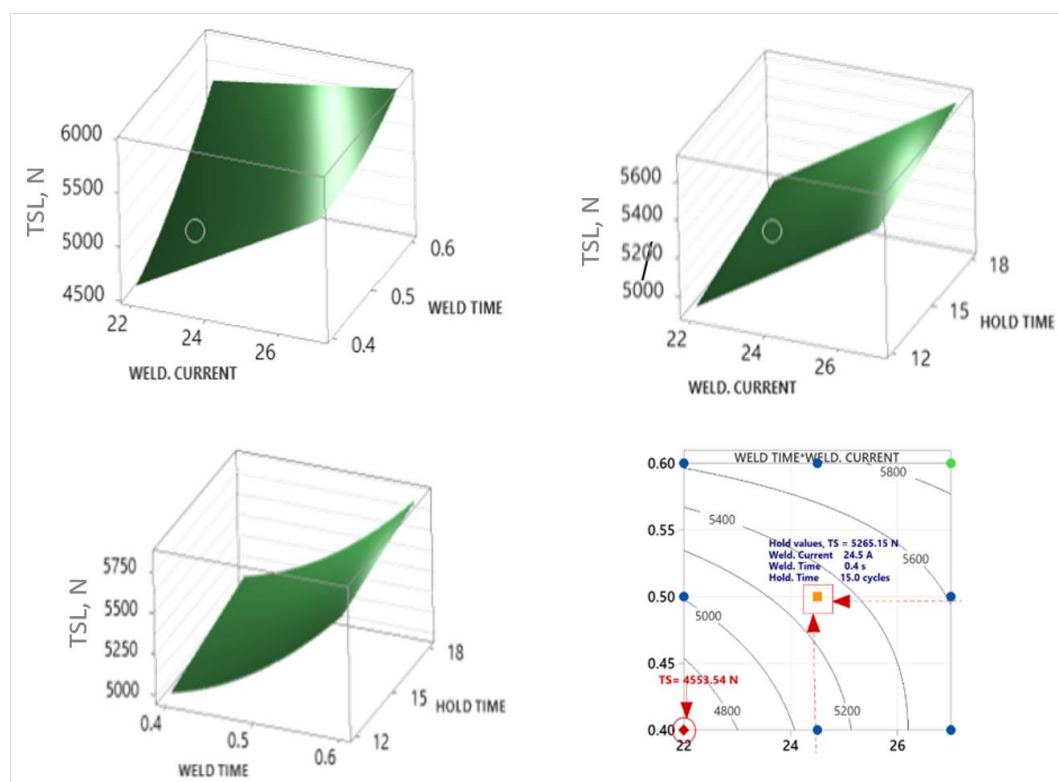


Figure 10.
The response surfaces of 27-iteration in tensile-share load

A contour plot is a useful visualization tool to understand the relationship between two input parameters and a response variable. It provides a two-dimensional model with contour lines of fixed responses connecting points with the same response. The contour plots were commonly used to explore desired response values and determine optimal operating conditions. The plots were employed in this study to examine the relationship between welding time and welding current, holding time and welding current, as well as holding time and welding time in order to optimize the TSL of the RSW technique. The contour plot showed the areas where the TSL was strongest using a bright green color and the best response values were found at the center of the plot as presented in Figure 11.

4. Conclusion

In conclusion, the optimization of the RSW TSL for dissimilar galvanized (SGCC) and non-galvanized steel (SPHC) using the response surface methodology (RSM) was successfully conducted. The optimal TSL value was achieved at a squeeze time of 21.0 cycles, welding current of 24.5 kA, welding time of 0.5 s, and holding time of 15.0 cycles. The highest TSL value was also recorded at 21.0 cycles, 27.0 kA, 0.6 s, and 15.0 cycles respectively. The welding current set above 0.4 kA allowed the prevention of interfacial failure mode. It was also discovered that the welding time could be adjusted to a longer duration to meet the desired current setting in cases where a

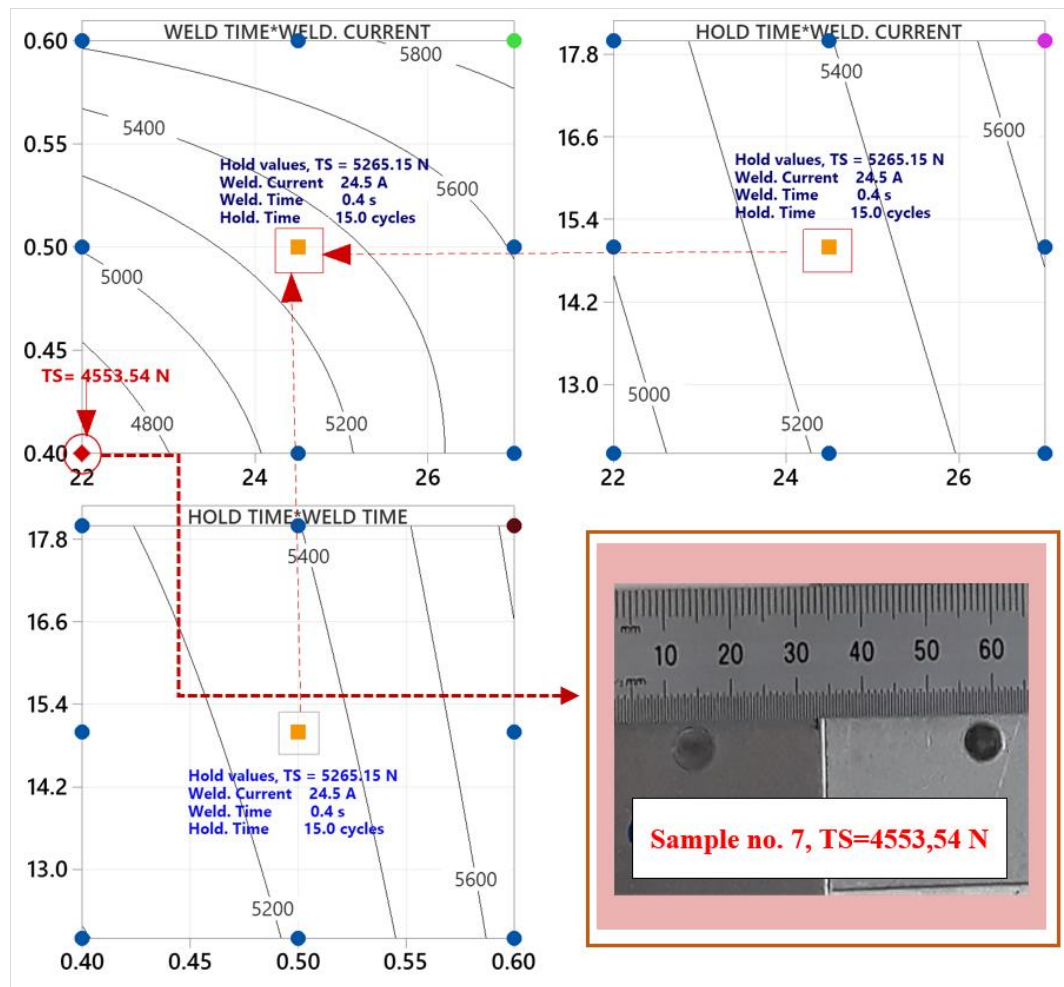


Figure 11.
The
counterplot of TSL in
dissimilar material RSW

welding current of 0.4 kA was applied. These findings provide and propose valuable input for optimizing the RSW process in order to achieve solid and reliable joints between galvanized and non-galvanized steel materials.

Acknowledgments

The author appreciates all the teams involved in this study, the staff of The University of Buana Perjuangan Karawang laboratory, and the PT Isaka Alindo Nusantara team for providing input and permission to use the RSW machine.

Authors' Declaration

Authors' contributions and responsibilities - The authors made substantial contributions to the conception and design of the study. The authors took responsibility for data analysis, interpretation, and discussion of results. The authors read and approved the final manuscript.

Funding –No funding information from the authors.

Availability of data and materials - All data are available from the authors.

Competing interests - The authors declare no competing interests.

Additional information – No additional information from the authors.

References

- [1] P. Russo Spena, M. De Maddis, F. Lombardi, and M. Rossini, "Investigation on Resistance Spot Welding of TWIP Steel Sheets," *Steel Research International*, vol. 86, no. 12, pp. 1480–1489, 2015, doi: 10.1002/srin.201400336.

- [2] S. Sukarman et al., "Optimal Tensile-Shear Strength Of Galvanized/Mild Steel (SPCC-SD) Dissimilar Resistance Spot Welding Using Taguchi DOE," *Jurnal Teknologi*, vol. 4, pp. 167–177, 2023.
- [3] S. K. Khanna, C. He, and H. N. Agrawal, "Residual stress measurement in spot welds and the effect of fatigue loading on redistribution of stresses using high sensitivity Moiré interferometry," *Journal of Engineering Materials and Technology, Transactions of the ASME*, vol. 123, no. 1, pp. 132–138, 2001, doi: 10.1115/1.1286218.
- [4] S. H. M. Anijdan, M. Sabzi, M. Ghobeiti-hasab, and A. Roshan-ghiyas, "Materials Science & Engineering A Optimization of spot welding process parameters in dissimilar joint of dual phase steel DP600 and AISI 304 stainless steel to achieve the highest level of shear-tensile strength," *Materials Science & Engineering A*, vol. 726, no. April, pp. 120–125, 2018, doi: 10.1016/j.msea.2018.04.072.
- [5] Posco, "Automotive," *Posco*, 2022. .
- [6] S. Sukarman, A. Abdulah, D. A. Rajab, and C. Anwar, "Optimization of Tensile-Shear Strength in the Dissimilar Joint of Zn-Coated Steel and Low Carbon Steel," *Automotive Experiences*, vol. 3, no. 3, pp. 115–125, 2020, doi: 10.31603/ae.v3i3.4053.
- [7] B. Xing, Y. Xiao, Q. H. Qin, and H. Cui, "Quality assessment of resistance spot welding process based on dynamic resistance signal and random forest based," *International Journal of Advanced Manufacturing Technology*, vol. 94, no. 1–4, pp. 327–339, 2018, doi: 10.1007/s00170-017-0889-6.
- [8] Miller Handbook, *Handbook for Resistance Spot Welding*. Miller Electric Mfg. Co., 2010.
- [9] E. Gunawan, S. Sukarman, A. D. Shieddieque, and C. Anwar, "Optimasi Parameter Proses Resistance Spot Welding pada Pengabungan Material SECC-AF," no. September, 2019.
- [10] D. L. Olson, S. Thomas A., S. Liu, and G. R. Edwards, *Welding, brazing, and soldering*, vol. 6. ASM International, 1990.
- [11] X. Wan, Y. Wang, and D. Zhao, "Multi-response optimization in small scale resistance spot welding of titanium alloy by principal component analysis and genetic algorithm," *International Journal of Advanced Manufacturing Technology*, vol. 83, no. 1–4, pp. 545–559, 2016, doi: 10.1007/s00170-015-7545-9.
- [12] M. K. Wahid, M. N. Muhammed Sufian, and M. S. Firdaus Hussin, "Effect of fatigue test on spot welded structural joint," *Jurnal Teknologi*, vol. 79, no. 5–2, pp. 95–99, 2017, doi: 10.11113/jt.v79.11290.
- [13] N. K. Singh and Y. Vijayakumar, "Application of Taguchi method for optimization of resistance spot welding of austenitic stainless steel AISI 301L," *Innovative Systems Design and Engineering*, vol. 3, no. 10, pp. 49–61, 2012.
- [14] A. H. Ertas and F. O. Sonmez, "Design optimization of spot-welded plates for maximum fatigue life," 2011, doi: 10.1016/j.fincl.2010.11.003.
- [15] H. Wiryosumarto and T. Okumura, *Teknologi Pengelasan Logam*, 8th ed. Jakarta: PT Pradnya Paramita, 2000.
- [16] J. P. Oliveira, K. Ponder, E. Brizes, T. Abke, A. J. Ramirez, and P. Edwards, "Combining resistance spot welding and friction element welding for dissimilar joining of aluminum to high strength steels," *Journal of Materials Processing Technology*, vol. 273, no. January, p. 116192, 2019, doi: 10.1016/j.jmatprotec.2019.04.018.
- [17] S. T. Pasaribu, S. Sukarman, A. D. Shieddieque, and A. Abdulah, "Optimasi Parameter Proses Resistance Spot Welding pada Pengabungan Bada Material SPCC," 2019, no. September.
- [18] A. G. Thakur and V. M. Nandedkar, "Optimization of the Resistance Spot Welding Process of Galvanized Steel Sheet Using the Taguchi Method," *Arabian Journal for Science and Engineering*, vol. 39, no. 2, pp. 1171–1176, 2014, doi: 10.1007/s13369-013-0634-x.
- [19] S. Shafee, B. B. Naik, and K. Sammaiah, "Resistance Spot Weld Quality Characteristics Improvement By Taguchi Method," *Materials Today: Proceedings*, vol. 2, no. 4–5, pp. 2595–2604, 2015, doi: 10.1016/j.matpr.2015.07.215.
- [20] H. E. Emre and R. Kaçar, "Development of weld lobe for resistance spot-welded TRIP800 steel and evaluation of fracture mode of its weldment," *International Journal of Advanced Manufacturing Technology, Springer*, vol. 85, pp. 1737–1747, 2016, doi: 10.1007/s00170-015-7605-1.
- [21] K. Vignesh, A. E. Perumal, and P. Velmurugan, "Optimization of resistance spot welding process parameters and microstructural examination for dissimilar welding of AISI 316L austenitic stainless steel and 2205 duplex stainless steel," *International Journal of Advanced Manufacturing Technology*, pp. 455–465, 2017, doi: 10.1007/s00170-017-0089-4.

- [22] V. Kuklík and J. Kudláček, *Hot-Dip galvanizing of steel structures*. 2016.
- [23] K. Khoirudin, S. Sukarman, N. Rahdiana, A. Suhara, and A. Fauzi, "Optimization of S-EDM Process Parameters on Material Removal Rate Using Copper Electrodes," *Jurnal Polimesin*, vol. 21, no. 1, pp. 17–20, 2023.
- [24] A. Abdulah and S. Sukarman, "OPTIMASI SINGLE RESPONSE PROSES RESISTANCE SPOT WELDING," *Multitek Indonesia: Jurnal Ilmiah*, vol. 6223, no. 2, pp. 69–79, 2020.
- [25] JIS G 3302, "JIS G 3302 Hot-dip zinc-coated steel sheet and strip." Japanese Industrial Standard, 2007.
- [26] JIS G3131, "Hot-rolled mild steel plates, sheet and strip." 2010.
- [27] American Welding Society, *Test Methods for Evaluating the Resistance Spot Welding Behavior of Automotive Sheet Steel (AWS D8.9M:2012)*. 2012, p. 7.
- [28] Miller Electric Mfg. Co., "Handbook for Resistance Spot Welding," 2012.
- [29] Y. G. Kim, D. C. Kim, and S. M. Joo, "Evaluation of tensile shear strength for dissimilar spot welds of Al-Si-Mg aluminum alloy and galvanized steel by delta-spot welding process," *Journal of Mechanical Science and Technology*, vol. 33, no. 11, pp. 5399–5405, 2019, doi: 10.1007/s12206-019-1034-2.
- [30] J. Pan and K. Sripichai, "Mechanics modeling of spot welds under general loading conditions and applications to fatigue life predictions," *Woodhead Publishing Limited*, 2010, doi: 10.1533/9781845699765.1.
- [31] Sukarman, C. Anwar, N. Rahdiana, and A. I. Ramadhan, "Analisis Pengaruh Radius Dies Terhadap Springback Logam Lembaran Stainless-Steel pada Proses Bending Hidrolik V-DIE," *Jurnal Teknologi*, vol. 12, no. 2, 2020.
- [32] P. J. Ross, *Taguchi Techniques for Quality Engineering*. New York: Tata McGraw-Hill, 2005.
- [33] H. Arjmandi, P. Amiri, and M. Saffari Pour, "Geometric optimization of a double pipe heat exchanger with combined vortex generator and twisted tape: A CFD and response surface methodology (RSM) study," *Thermal Science and Engineering Progress*, vol. 18, no. December 2019, p. 100514, 2020, doi: 10.1016/j.tsep.2020.100514.
- [34] P. G. Mathews, *Design of Experiments with MINITAB*, 12th ed., vol. 60, no. 2. Milwaukee: Mathews, Paul G., 2005.
- [35] F. A. Ghazali et al., *Three Response Optimization of Spot-Welded Joint Using Taguchi Design and Response Surface Methodology Techniques*, vol. 0. Springer Singapore, 2019.
- [36] R. Ribeiro, E. L. Romão, S. Costa, E. Luz, and J. H. Gomes, "Optimization of the resistance spot welding process of 22MnB5-galvannealed steel using response surface methodology and global criterion method based on principal components analysis," *Metals*, vol. 10, no. 10, pp. 1–25, 2020, doi: 10.3390/met10101338.
- [37] L. Jin-Hee, Bae.Yeong-Do, Park, Mokyoung, "Optimization of Welding Parameters for Resistance Spot Welding of AA3003 to Galvanized DP780 Steel Using Response Surface Methodology," *International Journal of Automotive Technology*, vol. 22, no. 3, pp. 585–593, 2021.